Asociación Argentina
de Mecánica Computacional

Mecánica Computacional Vol XXV, pp. 809-827
Alberto Cardona, Norberto Nigro, Victorio Sonzogni, Mario Storti. (Eds.)
Santa Fe, Argentina, Noviembre 2006

A FULLY COUPLED PARTICLE METHOD FOR QUASI-INCOMPRESSIBLE FLUID-HYPOELASTIC STRUCTURE INTERACTIONS

Julio Marti[a], Sergio Idelsohn[a,b], Alejandro Limache[a], Nestor Calvo[a] and Jorge D'Elía[a]

[a]*International Center for Computational Methods in Engineering (CIMEC),Universidad Nacional del Litoral and CONICET, Santa Fe, Argentina, email: jmarti@ceride.gov.ar*
[b]*International Center for Numerical Methods in Engineering (CIMNE), Universidad Politécnica de Cataluña, Barcelona, Spain*

Keywords: Particle finite element method, fluid-structure interaction, hypoelasticity.

Abstract. We present a general formulation for the simulation of fluid flows in interation with hypoelastic materials using the particle finite element method (PFEM). The fluid is fully coupled with the structures which can undergo large structural displacements, rotations and deformations. The key feature of the PFEM is the use of an updated Lagrangian description to model the motion of nodes (particles) in both the fluid and the structure domains. A mesh connects the nodes defining the discretized domains where the governing equations, expresed in an integral form, are solved as in the standard FEM. The implemented code is used to solve a number of fluid-structure interaction problems including free-fluid-surfaces and breaking waves impacting over hypoelastic structures.

1 INTRODUCTION

The analysis of multiphysics problems, and specifically the solution of fluid-structure interactions (FSI), has been given increased attention during recent years. There are many problems where a direct fully coupled analysis is needed to model the physics of FSI problem accurately. This is particularly the case when the structure undergoes large structural displacements, rotations and deformations in the interaction with the fluid. Examples of this kind are common in ship hydrodynamics, off-shore structures, spill-ways in dams, free surface channel flows, liquids containers, mould filling processes, etc.

In such case, the use of the ALE formulation (Donea and Huerta, 2006) is recommended to model the fluid domain and ease it coupling with the structural domain usually treated in the Lagrangian description. Generally, these problems are analyzed with the finite element method (FEM)(Zienkiewicz et al., 2006).

Typical difficulties of FSI analysis using the FEM include the treatment of the convective terms and the incompressibility constraint in the fluid equations, the modeling and tracking of the free surface in the fluid, the transfer of information between the fluid and solid domains via the interfaces analysis using, the modeling of wave splashing, the possibility to deal with large rigid body motions of the structure within the fluid domain, the efficient updating of the finite element meshes for both the structure and the fluid, etc.

Most of these problems disappear if a Lagrangian description of motion is used to formulate the governing equations of both the solid and the fluid domain. In the Lagrangian formulation, one essentially follows the history of individual particles and, consequently, nodes in a finite element mesh can be viewed as moving material point (called "particles"). Hence, the motion of the mesh discretizing the total domain (including both the fluid and solid parts) is followed during the transient solution.

In this paper, a Lagrangian formulation will be used together with a particular form of the FEM called the particle finite element method (PFEM) (Idelsohn et al., 2004b,a) to solve problems involving the interaction between fluids and solids in a unified manner. This approach allows to treat the fluid and the solid as a single entity, allowing to integrate in the time the two subdomains simultaneously (monolithic treatment). The PFEM, treats the mesh nodes in the fluid and solid domains as particles which can freely move and even separate from the main fluid domain representing, for instance, the effect of water drops. A finite element mesh connects the nodes defining the discretized domain where the governing equations are solved in the standard FEM fashion.

In the next section the basis of the Lagrangian and Eulerian descriptions are briefly presented. Next the constitutive equations are derived. Then the discretization of these equations in space and time is then discussed. Details of the basic ideas of the PFEM are outlined. Finally, numerical results in two dimensions problems are presented.

2 EQUATIONS OF MOTION

Neglecting thermomechanical effects, the motion of the elemental particles of any continuum material (fluid, solid or gas) can be determined by the equations of conservation of mass and momentum. These equations can be postulated as the continuum form of classical Newton's equations of motion and are independent of the material constitution or geometry. Using an Eulerian description, i.e. looking at the elemental particles as they pass through fixed positions in the physical space, the equations of conservation of mass and momentum can be stated in

local form as:

$$\frac{D\rho(\boldsymbol{x},t)}{Dt} = -\rho\left(\boldsymbol{x},t\right)\operatorname{div}\boldsymbol{V}\left(\boldsymbol{x},t\right) \tag{1}$$

$$\rho\left(\boldsymbol{x},t\right)\frac{D\boldsymbol{V}\left(\boldsymbol{x},t\right)}{Dt} = \operatorname{div}\sigma\left(\boldsymbol{x},t\right) + \rho\left(\boldsymbol{x},t\right)\mathbf{b}\left(\boldsymbol{x},t\right) \tag{2}$$

where $\sigma\left(\boldsymbol{x},t\right)$ is the Cauchy stress, and, $\rho\left(\boldsymbol{x},t\right)$ and $\boldsymbol{V}\left(\boldsymbol{x},t\right)$ are the density and the velocity vector of the elemental particles that at time t pass through the position $\boldsymbol{x}$, respectively. $\frac{D\phi}{Dt}$ denotes the total or material time-derivative of ϕ. In the absence of couple stresses the Cauchy stress is a second order symmetric tensor. In the Eulerian description the divergence div is taken with respect to the spatial coordinates $\boldsymbol{x}$. For example, div computed in cartesian coordinates $\boldsymbol{x} = x_k\boldsymbol{e}_k$ is:

$$\operatorname{div}\boldsymbol{V} = \frac{\partial V_k}{\partial x_k}$$

At any time t equations (1) and (2) can be solved on the whole volume Ω_t occupied by the material body, provided one knows the external body forces $\mathbf{b}$ (per unit of mass) and surface forces $\bar{\boldsymbol{t}}$ (see Figure 1).

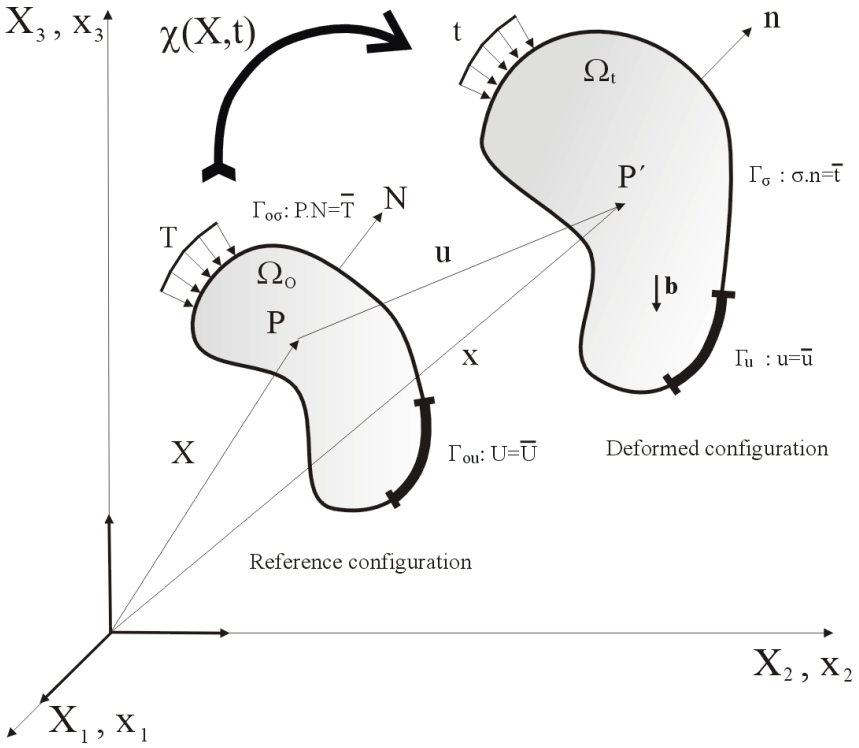

Figure 1: Movement of a deformable body

We can write equivalent conservation equations using a Lagrangian Formulation. In the Lagrangian description, one essentially follows the history of individual particles. Consequently, two independent variables are taken: the time t of evolution and a vector-type label associated to each particle. The label can be conveniently taken as the reference position vector $\boldsymbol{X}$ of the particle at some initial reference time $t = 0$. In this description, then, any quantity M is

expressed as $M = M(\boldsymbol{X}, t)$. In particular, the particle position is written as

$$\boldsymbol{x} = \boldsymbol{\chi}(\boldsymbol{X}, t) \tag{3}$$

which represents the location at t of the particle whose position was $\boldsymbol{X}$ at $t = 0$.

The knowledge of the deformation map χ for all the elemental particles completely defines the motion and deformation of the material body. In particular the velocities can be computed by:

$$\boldsymbol{V}(\boldsymbol{X}, t) = \frac{\partial \boldsymbol{\chi}(\boldsymbol{X}, t)}{\partial t} = \frac{D\boldsymbol{x}}{Dt} \tag{4}$$

Assuming the existence of the deformation map it is possible to rewrite the conservation equations (1) and (2) in terms of the reference coordinates $\mathbf{X}$:

$$\rho(\boldsymbol{x}, t) = \rho\left(\boldsymbol{\chi}(\boldsymbol{X}, t)\right) = \frac{\rho_0(\boldsymbol{X}, t)}{J(\boldsymbol{X}, t)} \tag{5}$$

$$\rho_0(\boldsymbol{X}, t)\frac{D\boldsymbol{V}(\boldsymbol{X}, t)}{Dt} = \mathrm{Div}\, \boldsymbol{P}(\boldsymbol{X}, t) + \rho_0 \boldsymbol{f}(\boldsymbol{X}, t) \tag{6}$$

where $\rho_0(\boldsymbol{X}, t)$ is the density of the material in the reference configuration, $J(\boldsymbol{X}, t)$ is the Jacobian

$$J(\boldsymbol{X}, t) = \det \boldsymbol{F}(\boldsymbol{X}, t) \tag{7}$$

of the deformation gradient

$$\boldsymbol{F}(\boldsymbol{X}, t) = \frac{\partial \boldsymbol{x}}{\partial \boldsymbol{X}} = \mathrm{Grad}(\boldsymbol{\chi}(\boldsymbol{X}, t)) \tag{8}$$

and $\boldsymbol{P}(\boldsymbol{X}, t)$ is the first Piola-Kirchhoff stress tensor

$$\boldsymbol{P}(\boldsymbol{X}, t) = J(\boldsymbol{X}, t)\boldsymbol{\sigma}(\boldsymbol{\chi}(\boldsymbol{X}, t)) \cdot \boldsymbol{F}^{-T}(\boldsymbol{X}, t) \tag{9}$$

Note that the differential operators divergence and gradient are written in lower-case letters $(\mathrm{div}, \mathrm{grad})$ when computed with respect to spatial coordinates x_k and in capital letters $(\mathrm{Div}, \mathrm{Grad})$ when computed with respect to material coordinates X_k.

From now on, we simplify the notation by writing the physical quantities without referencing their explicit dependence on time and on material or spatial coordinates. Then, the conservation equations (5) and (6) can be rewritten simply as:

$$\rho = \frac{\rho_0}{J} \tag{10}$$

$$\rho_0 \frac{D\boldsymbol{V}}{Dt} = \mathrm{Div}\, \boldsymbol{P} + \rho_0 \boldsymbol{f} \tag{11}$$

with the Jacobian given by:

$$J = \det \boldsymbol{F} \tag{12}$$

and the first Piola-Kirchhoff stress by:

$$\boldsymbol{P} = J\boldsymbol{\sigma} \cdot \boldsymbol{F}^{-T} \tag{13}$$

Observe that in the Lagrangian formulation, conservation of mass (10) is a direct consequence of a straightforward computation of the density in terms of the Jacobian and of the initial density

configuration ρ_0. The momentum equation has to be solved in conjunction with the boundary conditions representing the external loads and motion restrictions under which the material body is moving. In most of the cases one specifies surface forces $\boldsymbol{t}$ at certain surfaces Γ_σ of the boundary Γ of the body and impose prescribed displacements in the remaining parts $\Gamma_{\boldsymbol{U}}$ of the material's boundary:

$$\boldsymbol{\sigma} \cdot \boldsymbol{n} = \bar{\boldsymbol{t}} \quad \text{on} \quad \Gamma_{\boldsymbol{\sigma}} \tag{14}$$

$$\boldsymbol{U} = \bar{\boldsymbol{U}} \quad \text{on} \quad \Gamma_{\boldsymbol{U}} \tag{15}$$

Equations (10)-(15) are independent of the material, so we need to incorporate the information of the specific material we want to model. This is done by means of specifying the material's constitutive equation, which basically links the stress tensor to the deformation. In the context of the present paper we treat the problem of simulating incompressible newtonian fluids and isotropic hypoelastic solids either separately or in the form of a fluid-structure interaction. Accordingly in the next section we discuss their constitutive equations.

3 CONSTITUTIVE EQUATIONS

3.1 Constitutive Equation of Incompressible or Nearly-Incompressible Newtonian Fluids

We treat the incompressible fluid as the limit case of a nearly-incompressible newtonian flow. The constitutive equation of a newtonian fluid is a linear relationship between the Cauchy stress $\boldsymbol{\sigma}$ and the deformation rate tensor $\boldsymbol{D}$:

$$\boldsymbol{\sigma} = -p\boldsymbol{I} - \frac{2}{3}\mu_f(\operatorname{tr}\boldsymbol{D})\boldsymbol{I} + 2\mu_f\boldsymbol{D} \tag{16}$$

where μ_f is the fluid viscosity and p is the thermodynamic (or hydrostatic) pressure of the fluid. By definition $\boldsymbol{D}$ is the symmetric part

$$\boldsymbol{D} = \frac{1}{2}(\boldsymbol{L} + \boldsymbol{L}^T) \tag{17}$$

of the velocity gradient tensor:

$$\boldsymbol{L} = \operatorname{grad}\boldsymbol{V} \tag{18}$$

Note that:

$$\operatorname{tr}\boldsymbol{D} = \operatorname{div}\boldsymbol{V} = \boldsymbol{\varepsilon_v} \tag{19}$$

If $\boldsymbol{D}$ is decomposed in its volumetric and its deviatoric components:

$$\boldsymbol{D} = \left[\frac{1}{3}(\operatorname{tr}\boldsymbol{D})\boldsymbol{I} + \acute{\boldsymbol{D}}\right] = \left[\frac{1}{3}\varepsilon_v\boldsymbol{I} + \acute{\boldsymbol{D}}\right] \tag{20}$$

We can write (19) as:

$$\boldsymbol{\sigma} = -p\boldsymbol{I} + 2\mu_f\acute{\boldsymbol{D}} \tag{21}$$

Following Kundu and Cohen (2002), if the newtonian flow is nearly-incompressible then density changes are related to pressure changes by the following relationship:

$$dp = \frac{K_f}{\rho}d\rho \tag{22}$$

where K_f is the elastic bulk modulus of the fluid. Then applying the material time derivative to the equation above and using the equation of conservation of mass we get:

$$\frac{Dp}{Dt} = \frac{K_f}{\rho}\frac{D\rho}{Dt} = - \quad K_f \operatorname{div} \boldsymbol{V} \tag{23}$$

3.2 Time-Discretization of the Constitutive Equation of a Newtonian Fluid

A implicit discretization of the fluid's constitutive equation (21) is:

$$\boldsymbol{\sigma}^{(n+1)} = -p^{(n+1)}\boldsymbol{I} + 2\mu_f \acute{\boldsymbol{D}}^{(n+1)} \tag{24}$$

The discretized version of equation (23) for nearly incompressible flows would be:

$$\frac{p^{(n+1)} - p^{(n)}}{\triangle t} = \quad -K_f \operatorname{div}^{(n+1)} \boldsymbol{V}^{(n+1)} \tag{25}$$

So:

$$p^{(n+1)} = \quad p^{(n)} - \triangle t K_f \varepsilon_v^{(n+1)} \tag{26}$$

3.3 Constitutive Equation of Hypoelastic Solids

A isotropic hypoelastic solid (Truesdell and Noll, 1992) is a material whose constitutive equation is given by a linear isotropic relationship between the stress rate and the deformation rate:

$$\overset{\triangle}{\boldsymbol{\tau}} = 2\mu_h \boldsymbol{D} + \lambda_h (\operatorname{tr} \boldsymbol{D})\boldsymbol{I} \tag{27}$$

where $\overset{\triangle}{\boldsymbol{\tau}}$ is the Truesdell rate

$$\overset{\triangle}{\boldsymbol{\tau}} = \dot{\boldsymbol{\tau}} - \boldsymbol{L}\cdot\boldsymbol{\tau} - \boldsymbol{\tau}\cdot\boldsymbol{L}^T = \boldsymbol{F}\cdot\dot{\boldsymbol{S}}\cdot\boldsymbol{F}^T \tag{28}$$

of the Kirchhoff stress tensor $\boldsymbol{\tau} = J\boldsymbol{\sigma}$ and $\dot{\boldsymbol{S}}$ is the material time-derivative of the second Piola-Kirchhoff stress:

$$\boldsymbol{S} = \boldsymbol{F}^{-1}\cdot\boldsymbol{P} = J\boldsymbol{F}^{-1}\cdot\boldsymbol{\sigma}\cdot\boldsymbol{F}^{-T} \tag{29}$$

3.4 Time-discretization of the constitutive equation of an hypoelastic solid

A implicit discretization of the constitutive rate equation is:

$$\overset{\triangle}{\boldsymbol{\tau}}^{(n+1)} = 2\mu_h \boldsymbol{D}^{(n+1)} + \lambda_h (\operatorname{tr} \boldsymbol{D}^{(n+1)})\boldsymbol{I} \tag{30}$$

The Truesdell rate of the Kirchhoff stress is written within the interval as

$$\overset{\triangle}{\boldsymbol{\tau}}^{(n+1)} = \boldsymbol{F}^{(n+1)}\cdot\dot{\boldsymbol{S}}^{(n+1)}\cdot\boldsymbol{F}^{T(n+1)} \tag{31}$$

where $\boldsymbol{F}^{(n+1)}$ is the deformation gradient up to time $t^{(n+1)}$. Applying the generalized midpoint rule for $\dot{\boldsymbol{S}}^{(n+1)}$

$$\dot{\boldsymbol{S}}^{(n+1)} = \frac{\boldsymbol{S}^{(n+1)} - \boldsymbol{S}^{(n)}}{\triangle t} \tag{32}$$

we get

$$\boldsymbol{F}^{(n+1)} \cdot \left(\boldsymbol{S}^{(n+1)} - \boldsymbol{S}^{(n)} \right) \cdot \boldsymbol{F}^{T(n+1)} = 2\mu \triangle t \boldsymbol{D}^{(n+1)} + \lambda \triangle t (\mathrm{tr}\, \boldsymbol{D}^{(n+1)}) \boldsymbol{I} \tag{33}$$

using that $\boldsymbol{F} \cdot \boldsymbol{S} \cdot \boldsymbol{F}^T = J\boldsymbol{\sigma}$ and the so-called incremental deformation tensor $\boldsymbol{f}^{(n+1)}$ defined as:

$$\boldsymbol{f}^{(n+1)} \cdot \boldsymbol{F}^{(n)} = \boldsymbol{F}^{(n+1)} \tag{34}$$

we get:

$$J^{(n+1)} \boldsymbol{\sigma}^{(n+1)} = J^{(n)} \boldsymbol{f}^{(n+1)} \cdot \boldsymbol{\sigma}^{(n)} \cdot \boldsymbol{f}^{T(n+1)} + \lambda_h \triangle t (\mathrm{tr}\, \boldsymbol{D}^{(n+1)}) \boldsymbol{I} + 2\mu_h \triangle t \boldsymbol{D}^{(n+1)} \tag{35}$$

The equation (35) can be applied for both formulations. However in this paper we will use the Updated Lagrangian approach (see Section 4), then it suffices to replace $\boldsymbol{f}^{(n+1)}$ by $\boldsymbol{F}^{(n+1)}$ and $J^{(n)}$ by 1. Defining

$$\bar{\mu}_h^{(n+1)} = \frac{\mu_h \triangle t}{J^{(n+1)}}, \bar{\lambda}_h^{(n+1)} = \frac{\lambda_h \triangle t}{J^{(n+1)}} \tag{36}$$

and the tensor

$$\widehat{\boldsymbol{\sigma}}_h^{(n+1)} = \frac{1}{J^{(n+1)}} \boldsymbol{F}^{(n+1)} \cdot \boldsymbol{\sigma}^{(n)} \cdot \boldsymbol{F}^{T(n+1)} \tag{37}$$

we obtain the stress update expression:

$$\boldsymbol{\sigma}^{(n+1)} = \hat{\boldsymbol{\sigma}}_h^{(n+1)} + \bar{\lambda}_h^{(n+1)} (\mathrm{tr}\, \boldsymbol{D}^{(n+1)}) \boldsymbol{I} + 2\bar{\mu}_h^{(n+1)} \boldsymbol{D}^{(n+1)} \tag{38}$$

Decomposing the deformation rate tensor in terms of their deviatoric and volumetric part in the above equation, we obtain the following alternative expression:

$$\boldsymbol{\sigma}^{(n+1)} = \hat{\boldsymbol{\sigma}}_h^{(n+1)} + \left(\bar{\lambda}_h^{(n+1)} + \frac{2}{3} \bar{\mu}_h^{(n+1)} \right) (\boldsymbol{\varepsilon_v}^{(n+1)}) \boldsymbol{I} + 2\bar{\mu}_h^{(n+1)} \acute{\boldsymbol{D}}^{(n+1)} \tag{39}$$

Defining a hypoelastic volumetric viscosity:

$$\kappa_h = \bar{\lambda}_h + \frac{2}{3} \bar{\mu}_h \tag{40}$$

We get:

$$\boldsymbol{\sigma}^{(n+1)} = \hat{\boldsymbol{\sigma}}_h^{(n+1)} + \kappa_h^{(n+1)} \boldsymbol{\varepsilon_v}^{(n+1)} \boldsymbol{I} + 2\bar{\mu}_h^{(n+1)} \acute{\boldsymbol{D}}^{(n+1)} \tag{41}$$

If we decompose $\hat{\boldsymbol{\sigma}}_h^{(n+1)}$ in its deviatoric and volumetric part

$$\hat{\boldsymbol{\sigma}}_h^{(n+1)} = -\hat{p}_h^{(n+1)} \boldsymbol{I} + \acute{\hat{\boldsymbol{\sigma}}}_h^{(n+1)} \tag{42}$$

We have:

$$\boldsymbol{\sigma}^{(n+1)} = -\hat{p}_h^{(n+1)} + \kappa_h^{(n+1)} \boldsymbol{\varepsilon_v}^{(n+1)} \boldsymbol{I} + 2\bar{\mu}_h^{(n+1)} \acute{\boldsymbol{D}}^{(n+1)} + \acute{\hat{\boldsymbol{\sigma}}}_h^{(n+1)} \tag{43}$$

From the application of the trace operator to the equation above we get the following useful relationship:

$$p^{(n+1)} = \hat{p}_h^{(n+1)} - \kappa_h^{(n+1)} \boldsymbol{\varepsilon_v}^{(n+1)} \tag{44}$$

where $p^{(n+1)}$ is the mean pressure:

$$p = -\frac{1}{3} \operatorname{tr} \boldsymbol{\sigma}$$

of the stress tensor $\boldsymbol{\sigma}^{(n+1)}$. Then,

$$\boldsymbol{\sigma}^{(n+1)} = -p^{(n+1)} \boldsymbol{I} + 2\bar{\mu}_h^{(n+1)} \acute{\boldsymbol{D}}^{(n+1)} + \acute{\hat{\boldsymbol{\sigma}}}_h^{(n+1)} \tag{45}$$

This is a discrete version of the constitutive equation of an hypoelastic material.

3.5 A unique constitutive formulation for a Newtonian Fluid and a Hypoelastic Solid

Now we make use of the similarity between the constitutive equation of the hypoelastic solid (45) and the constitutive equation of a Newtonian fluid (24) so as to write a unique constitutive equation for both materials. The only differences between the constitutive equations are the additional term $\acute{\hat{\boldsymbol{\sigma}}}_h^{(n+1)}$ for the hypoelastic solid and the fact that their Lamé Coefficients are not longer constant. As a consequence we can write the following general expressions for both materials:

$$\boldsymbol{\sigma}^{(n+1)} = -p^{(n+1)} \boldsymbol{I} + 2\mu^{(n+1)} \acute{\boldsymbol{D}}^{(n+1)} + \acute{\hat{\boldsymbol{\sigma}}}^{(n+1)} \tag{46}$$

with

$$p^{(n+1)} = \hat{p}^{(n+1)} - \mathcal{K} \boldsymbol{\varepsilon_v}^{(n+1)} \tag{47}$$

where

$$\mu^{(n+1)} = \begin{cases} \bar{\mu}_h = \frac{\mu_h \triangle t}{J^{(n+1)}} & \text{if Hypoelastic solid} \\ \mu_f^{(n+1)} & \text{if Newtonian fluid} \end{cases}$$

$$\widehat{p}^{(n+1)} = \begin{cases} \hat{p}_h^{(n+1)} & \text{if Hypoelastic solid} \\ p^{(n)} & \text{if Newtonian fluid} \end{cases}$$

$$\mathcal{K} = \begin{cases} \frac{\lambda_h \triangle t}{J^{(n+1)}} + \frac{2}{3} \frac{\mu_h \triangle t}{J^{(n+1)}} & \text{if Hypoelastic solid} \\ \triangle t K_f & \text{if Newtonian fluid} \end{cases}$$

$$\hat{\boldsymbol{\sigma}}^{(n+1)} = \begin{cases} \frac{1}{J^{(n+1)}} \boldsymbol{F}^{(n+1)} \cdot \boldsymbol{\sigma}^{(n)} \cdot \boldsymbol{F}^{T(n+1)} & \text{if Hypoelastic solid} \\ p^{(n)} \boldsymbol{I} & \text{if Newtonian fluid} \end{cases} \tag{48}$$

$$\acute{\hat{\boldsymbol{\sigma}}}^{(n+1)} = \begin{cases} \acute{\hat{\boldsymbol{\sigma}}}_h^{(n+1)} & \text{if Hypoelastic solid} \\ 0 & \text{if Newtonian fluid} \end{cases}$$

4 TIME-DISCRETIZATION OF EQUATIONS OF MOTION USING A LAGRANGIAN FORMULATION

To obtain numerical solutions to equations (10)-(15) we use a Lagrangian Formulation. The formulation can be made either Total Lagrangian or Updated Lagrangian. In the former the reference configuration is the initial one, in the second the reference configuration is chosen to be the most recent computated configuration and it is updated every time step. In this paper we will use the Updated Lagrangian approach only. Having chosen a reference configuration which corresponds to a volume Ω_0 with a density distribution ρ_0, applying the Newmark method (Newmark (1959)) to integrate in the time the equations (10) and (11) leads to:

$$\rho_0 \frac{\mathbf{V}^{(n+1)} - \mathbf{V}^{(n)}}{\Delta t} = \text{Div}\left(J^{(n+1)}\boldsymbol{\sigma}^{(n+1)} \cdot \boldsymbol{F}^{-T(n+1)}\right) + \rho_0 \boldsymbol{b}^{(n+1)} \tag{49}$$

with

$$\rho^{(n+1)} = \frac{1}{J^{(n+1)}}\rho_0 \tag{50}$$

where

$$\boldsymbol{U}^{(n+1)} = \boldsymbol{U}^{(n)} + \Delta t \boldsymbol{V}^{(n)} + \Delta t^2 \left((\frac{1}{2} - \beta)\boldsymbol{A}^{(n)} + \beta \boldsymbol{A}^{(n+1)}\right) \tag{51}$$

$$\boldsymbol{V}^{(n+1)} = \boldsymbol{V}^{(n)} + \Delta t \left((1-\gamma)\boldsymbol{A}^{(n)} + \gamma \boldsymbol{A}^{(n+1)}\right) \tag{52}$$

The values of γ and β determine the order of the method. However, the order of the method is limited to 1 so that values of $\gamma = 1$ and $\beta = 0.5$ are chosen. The above equations are solved in the reference volume Ω_0 and the boundary conditions imposed on the reference volume's boundary $\Gamma_0 = \Gamma_{0\boldsymbol{U}} + \Gamma_{0\boldsymbol{\sigma}}$.

Equations (10)-(15) or their discrete form (49)-(50) are independent of the material, so we need to incorporate the materialt's constitutive equations. In the context of the present paper we treat the problem of simulating quasi-incompressible newtonian fluids and isotropic hypoelastic solids either separately or in the form of a fluid-structure interaction.

5 INTEGRATION OF MOTION EQUATIONS

Inserting the general constitutive equation (46) into equation (49) and assuming an Updated Lagrangian Approach (i.e. $\rho_0 = \rho^{(n)}$) we get:

$$\rho^{(n)}\left(\frac{\boldsymbol{V}^{(n+1)} - \boldsymbol{V}^{(n)}}{\Delta t}\right) = -\text{Div}\left(J^{(n+1)}p^{(n+1)}\boldsymbol{I} \cdot \boldsymbol{F}^{-T(n+1)}\right) + \text{Div}\left(J^{(n+1)}2\mu^{(n+1)}\acute{\boldsymbol{D}}^{(n+1)} \cdot \boldsymbol{F}^{-T(n+1)}\right) + \text{Div}\left(J^{(n+1)}\acute{\hat{\boldsymbol{\sigma}}}^{(n+1)} \cdot \boldsymbol{F}^{-T(n+1)}\right) + \rho^{(n)}\boldsymbol{b}^{(n+1)} \tag{53}$$

Now in order to ease readiness, we will drop the upper-index $(n+1)$ from the unknown quantities. So for example $\boldsymbol{F}^{-T(n+1)}$ will be written simply as $\boldsymbol{F}^{-T}$. Note that we keep the index (n) of the known quantities. Using this convention we can rewrite the above equation as:

$$\rho^{(n)}\left(\frac{\boldsymbol{V} - \boldsymbol{V}^{(n)}}{\Delta t}\right) = -\text{Div}\left(Jp\boldsymbol{I} \cdot \boldsymbol{F}^{-T}\right) + \text{Div}\left(J2\mu\acute{\boldsymbol{D}} \cdot \boldsymbol{F}^{-T}\right) + \text{Div}\left(J\acute{\hat{\boldsymbol{\sigma}}} \cdot \boldsymbol{F}^{-T}\right) + \rho^{(n)}\boldsymbol{b} \tag{54}$$

Using (47), we have:

$$\rho^{(n)}\left(\frac{\boldsymbol{V}-\boldsymbol{V}^{(n)}}{\Delta t}\right) = -\operatorname{Div}\left(J\hat{p}\boldsymbol{I}\cdot\boldsymbol{F}^{-T}\right)+\operatorname{Div}\left(J\mu\left(\operatorname{grad}\boldsymbol{V}+\operatorname{grad}^{T}\boldsymbol{V}\right)\cdot\boldsymbol{F}^{-T}\right)+ \operatorname{Div}\left(J\left(\mathcal{K}-\frac{2}{3}\mu\right)\varepsilon_{v}\boldsymbol{I}\cdot\boldsymbol{F}^{-T}\right)+\operatorname{Div}\left(J\hat{\boldsymbol{\sigma}}\cdot\boldsymbol{F}^{-T}\right)+\rho^{(n)}\boldsymbol{b} \tag{55}$$

5.1 Spatial Discretization

Multiplying equation (55) by the test function W and (47) by q and integrating over the domain, we arrive at :

$$\int_{\Omega_n}\rho^{(n)}\boldsymbol{W}\cdot\left(\frac{\boldsymbol{V}-\boldsymbol{V}^{(n)}}{\Delta t}\right)dV_n = \int_{\Omega_n}\boldsymbol{W}\cdot(-\operatorname{Div}\left(J\hat{p}\boldsymbol{I}\cdot\boldsymbol{F}^{-T}\right)+\operatorname{Div}\left(J\mu\left(\operatorname{grad}\boldsymbol{V}+\operatorname{grad}^{T}\boldsymbol{V}\right)\cdot\boldsymbol{F}^{-T}\right)+ \operatorname{Div}\left(J\left(\mathcal{K}-\frac{2}{3}\mu\right)\varepsilon_{v}\boldsymbol{I}\cdot\boldsymbol{F}^{-T}\right)+ \operatorname{Div}\left(J\hat{\boldsymbol{\sigma}}\cdot\boldsymbol{F}^{-T}\right)+\rho^{(n)}\boldsymbol{b})dV_n+\int_{\Gamma_n}\boldsymbol{W}(\boldsymbol{T}-\boldsymbol{P}\cdot\boldsymbol{N})d\Gamma_n \tag{56}$$

$$\int_{\Omega_n}qp^{(n+1)}\,dV_n=\int_{\Omega_n}q\left(\hat{p}^{(n+1)}\;-\mathcal{K}\boldsymbol{\varepsilon_v}^{(n+1)}\right)dV_n \tag{57}$$

After integration by parts, equation (56) becomes:

$$\int_{\Omega_n}\rho^{(n)}\boldsymbol{W}\cdot\left(\frac{\boldsymbol{V}-\boldsymbol{V}^{(n)}}{\Delta t}\right)dV_n=\int_{\Omega_n}\operatorname{Grad}\boldsymbol{W}:(J\hat{p}\boldsymbol{I}\cdot\boldsymbol{F}^{-T})dV_n- \int_{\Omega_n}\operatorname{Grad}\boldsymbol{W}:(J\mu\left(\operatorname{Grad}\boldsymbol{V}+\operatorname{Grad}^{T}\boldsymbol{V}\right)\cdot\boldsymbol{F}^{-1}\cdot\boldsymbol{F}^{-T})dV_n- \int_{\Omega_n}\operatorname{Grad}\boldsymbol{W}:\left(J\left(\mathcal{K}-\frac{2}{3}\mu\right)\varepsilon_{v}\boldsymbol{I}\cdot\boldsymbol{F}^{-T}\right)dV_n-\int_{\Omega_n}\operatorname{Grad}\boldsymbol{W}:(J\hat{\boldsymbol{\sigma}}\cdot\boldsymbol{F}^{-T})dV_n+ \int_{\Omega_n}\rho^{(n)}\boldsymbol{W}\cdot\boldsymbol{b}dV_n+\int_{\Gamma_n}\boldsymbol{W}\cdot\boldsymbol{T}d\Gamma_n \tag{58}$$

The velocity and the pressure are approximated as:

$$V_j=\sum W_i\left(X,t\right)V_{i,j}$$
$$p=\sum W_i\left(X,t\right)P_i \tag{59}$$

where W_i are the MFEM shape functions and $\boldsymbol{V}$ and p the nodal values of the three components of the unknown velocity and the pressure respectively. More details of the mesh discretization process and the choice of shape functions are given in section 8. Substituting the

approximation (59) into (57)-(58) and choosing a Galerkin method leads to the following systems of equations:

$$(\boldsymbol{M} + \Delta t \boldsymbol{K})\, V = \boldsymbol{M} V^{(n)} - \Delta t \boldsymbol{D}\hat{\boldsymbol{\sigma}} + \Delta t \boldsymbol{D}\hat{p} + \Delta t \boldsymbol{F} \tag{60}$$

$$\widehat{\boldsymbol{M}} p = \widehat{\boldsymbol{M}}\hat{p} - \boldsymbol{G} V \tag{61}$$

where the previous matrices are:

$$K_{ij} = \int_{\Omega_n} \operatorname{Grad} W_i \boldsymbol{F}^{-1} \mu \left(\operatorname{Grad} W_j + \operatorname{Grad}^T W_j\right) \boldsymbol{F}^{-1} J dV_n + \int_{\Omega_n} \operatorname{Grad} W_i \boldsymbol{F}^{-T} \left(\mathcal{K} - \frac{2}{3}\mu\right) \operatorname{Grad} W_j \boldsymbol{F}^{-T} J dV_n \tag{62}$$

$$M_{ij} = \int_{\Omega_n} \rho^{(n)} W_i W_j dV_n \qquad \widehat{M_{ij}} = \int_{\Omega_n} W_i W_j dV_n \tag{63}$$

$$D_{ij} = \int_{\Omega_n} \operatorname{Grad} W_i W_j \boldsymbol{F}^{-T} J dV_n \qquad G_{ij} = \int_{\Omega_n} W_i \mathcal{K} \operatorname{Grad} W_j \boldsymbol{F}^{-T} dV_n \qquad F_i = \int_{\Omega_n} W_i \boldsymbol{b} dV_n + \int_{\Gamma_n} W_i \boldsymbol{T} d\Gamma_n \tag{64}$$

6 SUMMARY OF A FULL ITERATIVE TIME STEP

The resulting nonlinear system of equations (60)-(61) has to be solved iteratively. Therefore, a Picard iteration is used for the linearization of all equations, leading to a relatively simple fixed point type solution procedure. A full time step may be described as follows: starting with the known values $\boldsymbol{X}^{(n)}$, $\boldsymbol{V}^{(n)}$ and $\boldsymbol{\sigma}^{(n)}$ in each particle, the computation of the new particle position involve the following steps:

1- Initialize $\boldsymbol{F}^{(n+1,0)} = \delta_{ij}\boldsymbol{ei} \otimes \boldsymbol{ej}$,$J^{(n+1,0)} = 1$, $\boldsymbol{x}^{(n+1,0)} = \boldsymbol{X}^{(n)}$
2- While (not converge)
a)Evaluate the velocity $\boldsymbol{V}^{(n+1,i+1)}$

$$(\boldsymbol{M} + \Delta t \boldsymbol{K})\, V^{(n+1,i+1)} = \boldsymbol{M} V^{(n)} - \Delta t \boldsymbol{D}\hat{\boldsymbol{\sigma}}^{(n+1)} + \Delta t \boldsymbol{D}\hat{p}^{(n+1)} + \Delta t \boldsymbol{F}^{(n+1)} \tag{65}$$

d)Move the particles to the $x^{(n+1,i+1)}$ position with

$$\boldsymbol{x}^{(n+1,i+1)} = \boldsymbol{X}^{(n)} + \boldsymbol{U}^{(n+1,i+1)} \tag{66}$$

e)Compute the deformation gradient $\boldsymbol{F}^{(n+1,i+1)}$ from (8) and $J^{(n+1,i+1)}$ from (7)
3-If converge

4. Solve the coupled Lagrangian equation of motion for the fluid and the solid domains. Compute the relevant state variables in both domains at the next (updated) configuration for $t+\Delta t$: velocities, pressure and viscous stresses in the fluid and displacements, stresses and strains in the solid.

5. Move the mesh nodes to a new position C^{n+1} where $n+1$ denotes the time $t_n + \Delta t$, in terms of the time increment size. This step is typically a consequence of the solution process of step 4.

6. Go back to step 1 and repeat the solution process for the next time step.

8 MESH GENERATION

A key point for the success of the Lagrangian FSI formulation is the fast regeneration of a mesh at every time step on the basis of the position of the nodes in the space domain. The mesh is generated using the so called extended Delaunay tesselation (EDT) presented in (Idelsohn et al., 2003b,a; Edelsbrunner and Mucke, 1999). The C^0 continuous shape functions of the elements can be simply obtained using the so called meshless finite element interpolation (MFEM). Details of the mesh generation procedure and derivation of the MFEM shape functions can be found in (Idelsohn et al., 2003b,a; Edelsbrunner and Mucke, 1999). One of the main problems in mesh generation is the correct definition of the boundary domain. The use of the extended Delaunay partition makes it easier to recognize boundary nodes.

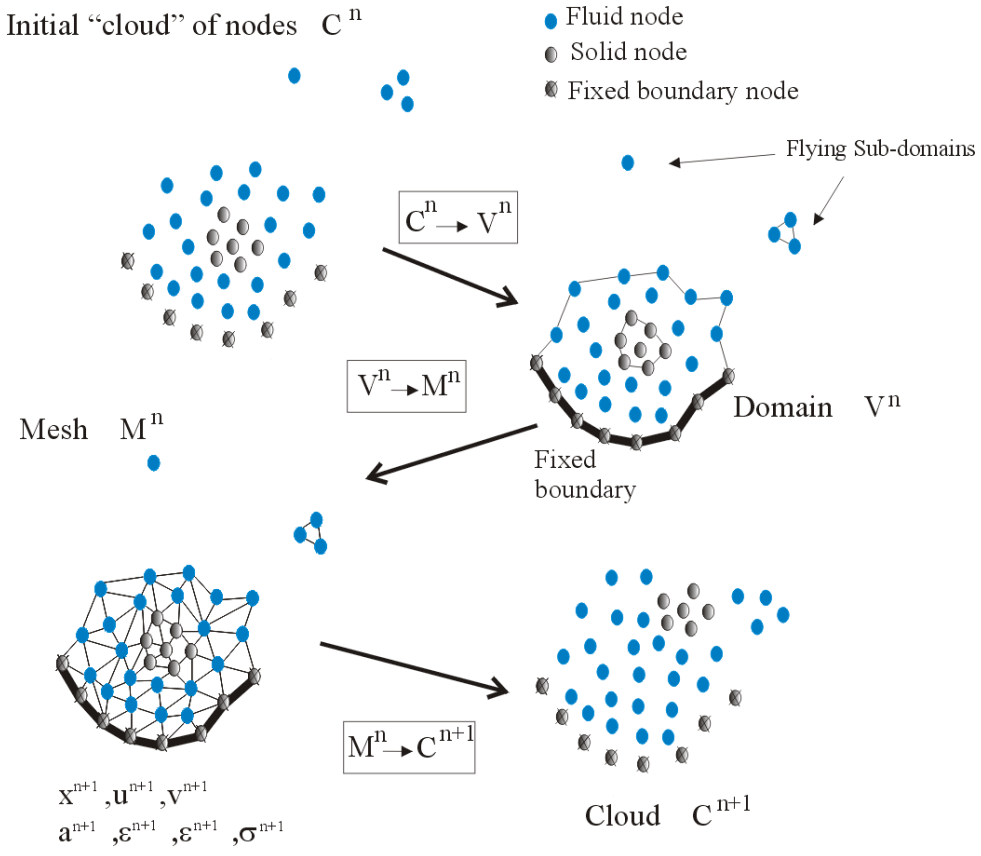

Figure 2: Sequence of steps to update a "cloud" of nodes from time n (time n) to time n+1 (t=tn+Δt)

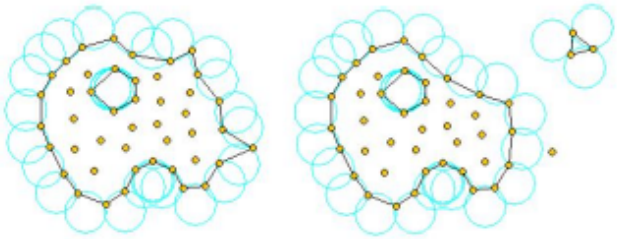

Figure 3: Identification of individual particles (or a group of particles) starting from a given collection of nodes

Considering that the particles follow a variable $h(x)$ distribution, where $h(x)$ is the minimum distance between two particles, the following criterion has been used: All particles on an empty sphere with a radius $r(x)$ bigger than $h(x)$, are considered as boundary nodes. α is a parameter close to, but greater than one. Note that this criterion is coincident with the Alpha Shape concept (Edelsbrunner and Mucke, 1999). Figure 3 shows an example of the boundary recognition using the Alpha Shape technique.
In this work, the boundary surface is defined by all the polyhedral surfaces (or polygons in 2D) having all their nodes on the boundary and belonging to just one polyhedron.
The method described also allows one to identify isolated fluid particles outside the main fluid domain.

9 EXAMPLES

9.1 Collapse of a water column with a obstacle

The collapse of a water column is calculated using the present formulation and results compared with experiment results obtained by S. Koshizuka in reference (Koshizuka et al., 1995). Geometry of the initial water column is illustrated in Figure 4. The fluid properties correspond to water, so that $\rho = 1000[kg/m^3]$ and $\mu = 0.001[kg/sm]$. The system is simulated for $2[s]$ with a time steps $= 0.0025[s]$. Figure 5 show the experimental and the numerical results at different characteristic time step. At time $0.1[s]$, the right surfaces of the water start the disturbance due to the obstacle. At time $0.2[s]$, the water surface is completely disturbed by the obstacle.

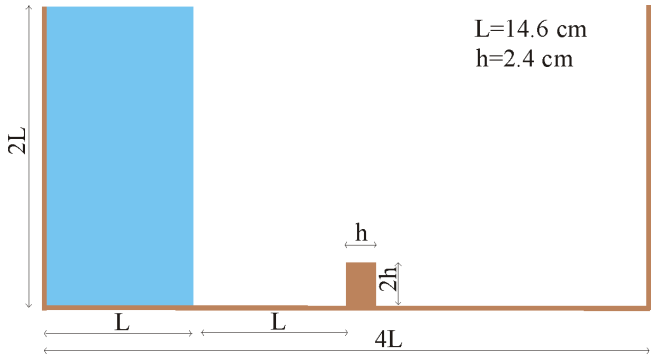

Figure 4: Initial geometry of the water column

The results compare considerably well with the experimental results. At $0.3[s]$ collapsed water crashes to the right wall. At $0.5[s]$, the water goes up along the right wall with separations

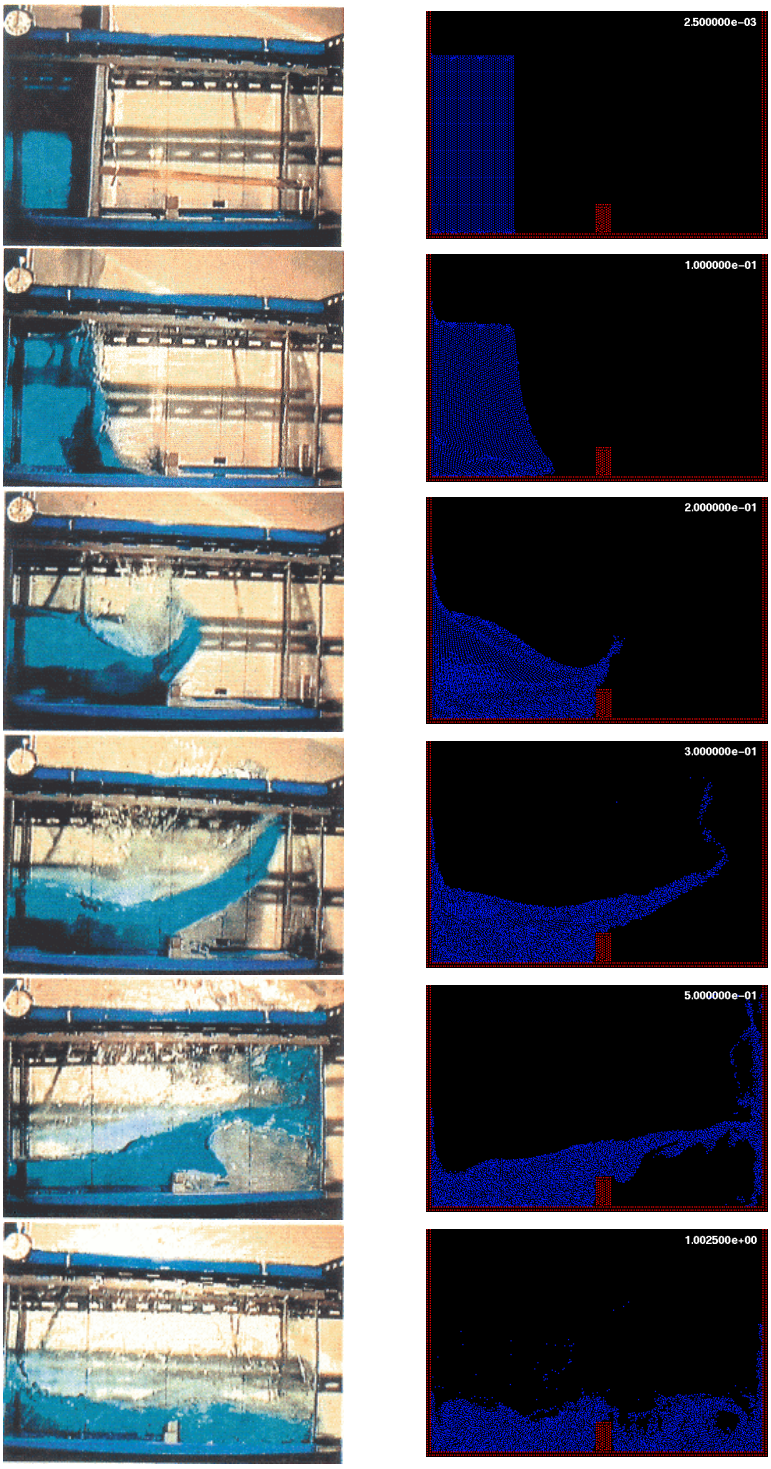

Figure 5: Collapsing water column with obstacle

and several drops. Finally, at $1[s]$, the water along the right wall falls down and a new breaking wave will soon occur on the left wall.

9.2 Breaking dam on hypoelastic wall

Figure 6 represents the same problem but with a elastic obstacle with density $\rho = 2500[kg/m^3]$, Young's modulus $E = 10^6[kg/s^2m]$ and Poisson's ratio $\nu = 0$. The geometry of the more slender obstacle is of width $h = 1.2[cm]$ and height $20/3 \cdot h$. No experimental results have been found for this example, but the shape of the deformation of the beam as well as the free surface perturbation seems to be in agreement with the physics of the problem.

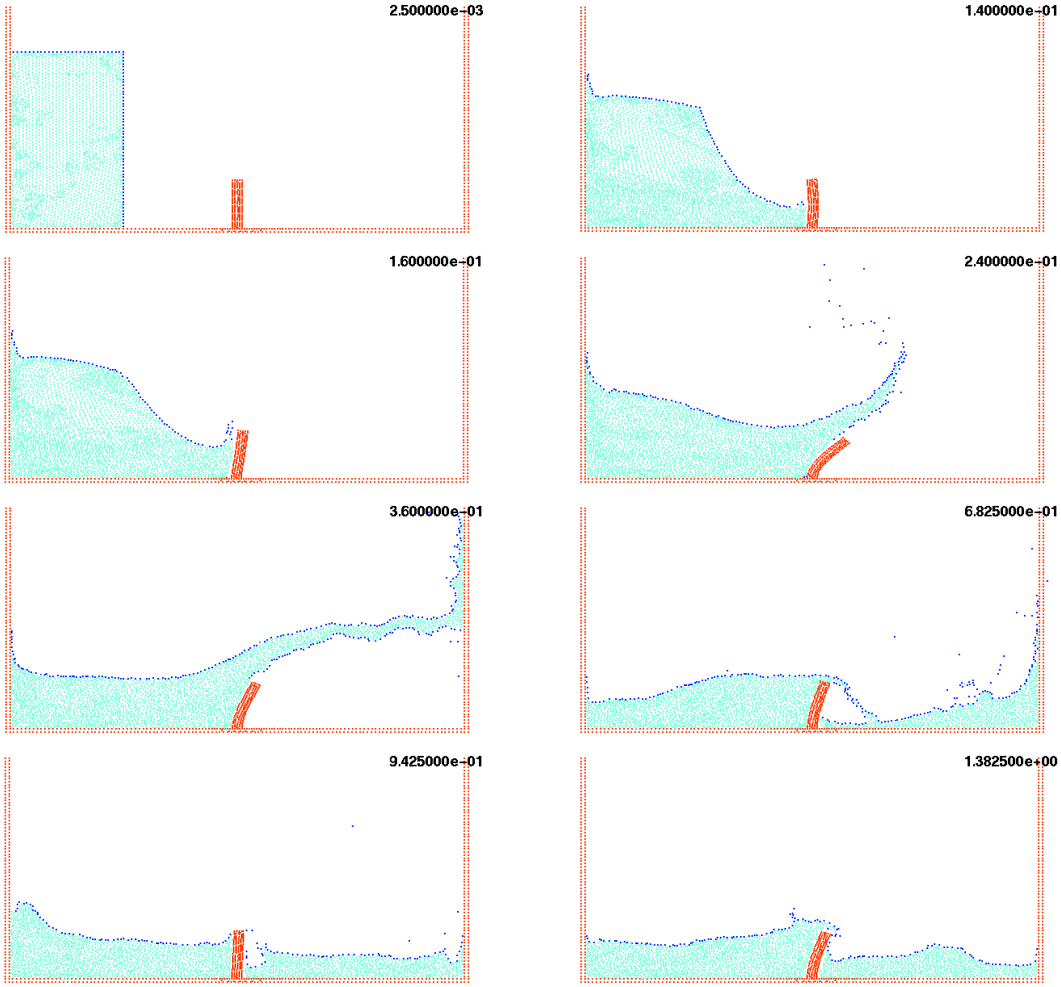

Figure 6: Breaking dam on hypoelastic

The left upper corner of the solid first gets a defection to the left when the water acts on its lower part and moves to the right while the water rises. It obtains its maximum deflection (mark (a) in Figure 7) when the water jet passes the top and is fully attached to the left side of the solid. Finally, the impact of the fluid causes the thin solid to start oscillating (b). This oscillation is damped (c) by the water located left and right of the wall.

9.3 Bar under a lateral wave

In this example a bar is located in the middle of a tank. The obstacle with density $\rho = 7800[kg/m^3]$, Young's modulus $E = 2.1 \cdot 10^6[kg/s^2m]$ and Poisson's ratio $\nu = 0.3$. Geometry is illustrated in Figure 8.

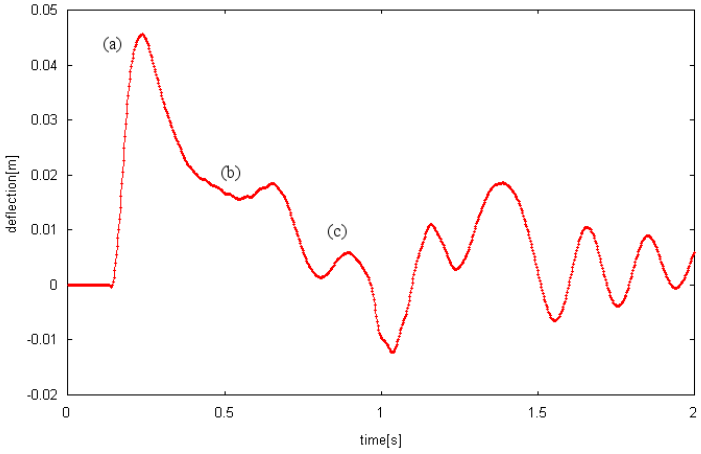

Figure 7: History of the displacement

Now, the system is simulated for $2[s]$ with a constant time step $= 0.001[s]$. The hypoelastic solid is deflected by the impulse of the fluid wave (Figure 9). The the solid first moves to the left while the water rises and to the right when the wave goes back.

10 CONCLUSIONS

In this paper, the Particle Finite Element Method applied to solve Fluid-Structure Interaction problems in a monolithic numerical scheme was presented. The method takes advantage of the similarity between the discrete constitutive equations of the materials under consideration: quasi-incompressible newtonian fluid and hypoelastic solid, and it has proved to be ideal to treat problems involving fluid with free surfaces and structures which can undergo large structural displacements, rotations and deformations. Other, essential solution ingredients of the numerical approach are: the Delaunay triangulation algorithm which provides a very efficient connectivity scheme, and, the identification of boundary nodes using an Alpha-Shape type technique. The examples presented have shown the great potential of the PFEM for solving a wide class of practical FSI problems.

REFERENCES

J. Donea and A. Huerta. *Finite element method for flow problems*. J.Willey, 2006.
H. Edelsbrunner and E.P. Mucke. *Three dimensional alpha shapes. ACM Trans. Graphics.*, 13:

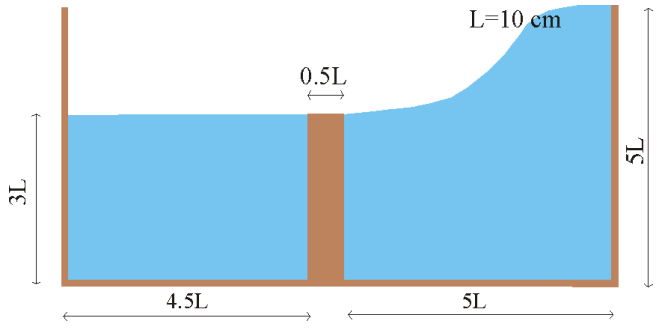

Figure 8: Initial geometry of the bar under a lateral wave

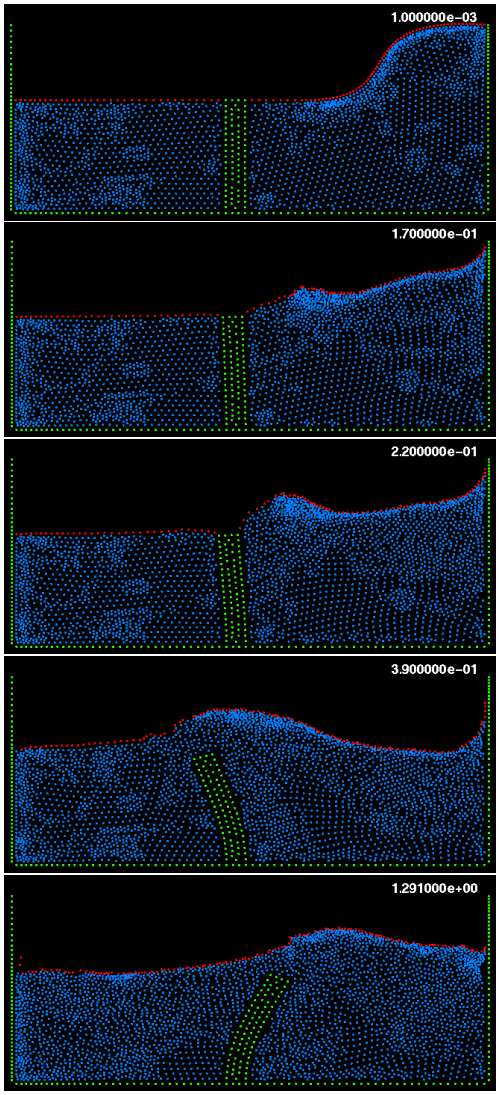

Figure 9: Bar under a lateral wave

43–72, 1999.

S. Idelsohn, N. Calvo, and E. Oñate. Polyhedrization of an arbitrary point set. *Comput. Method Appl. Mech. Engng.*, 192:2648–2668, 2003a.

S. Idelsohn, F. Del Pin, and R. Aubry. The particle finite element method: an overview. *Int. J. Computat. Methods*, 2:267–307, 2004a.

S. Idelsohn, E. Oñate, N. Calvo, and F.Del Pin. The meshless finite element method. *Int. J. Num. Meth. Engng.*, 58:(6)893–912, 2003b.

S. Idelsohn, E. Oñate, and F. Del Pin. The particle finite element method: a powerful tool to solve incompressible flows with free-surfaces and breaking waves. *Int. J. Num. Meth. Engng.*, 61:(7)964–989, 2004b.

S. Koshizuka, H. Tamko, and Y. Oka. A particle method for incompressible viscous flow with fluid fragmentation. *Comput. Fluid Dynamic Journal*, 1:29–46, 1995.

P.K. Kundu and I.M. Cohen. *Fluid Mechanics*. Academic Press, 2002.

N.M. Newmark. A method of computation for structural dynamics. *Proc. A.S.C.E.*, 8:67–94, 1959.

C.A. Truesdell and W. Noll. *The non-linear field theories of mechanics,Handbuch der Physik*, volume Bd III/3. Springer,Berlin, 1992.

O.C. Zienkiewicz, R.L. Taylor, and P. Nithiarasu. The finite element method for fluid dynamics. *Elsevier*, 2006.